

# Significant negative differential resistance predicted in scanning tunneling spectroscopy for a C<sub>60</sub> monolayer on a metal surface

X. Q. Shi,<sup>1</sup> Woei Wu Pai,<sup>2</sup> X. D. Xiao,<sup>3</sup> J. I. Cerdá,<sup>4</sup> R. Q. Zhang,<sup>1</sup> C. Minot,<sup>1,5</sup> and M. A. Van Hove<sup>1</sup>

<sup>1</sup>*Department of Physics and Materials Science, City University of Hong Kong, Kowloon, Hong Kong, SAR, China*

<sup>2</sup>*Center for Condensed Matter Sciences, National Taiwan University, Taipei 106, Taiwan*

<sup>3</sup>*Department of Physics, Chinese University of Hong Kong, Shatin, Hong Kong, SAR, China*

<sup>4</sup>*ICMM-CSIC, Cantoblanco, 28049 Madrid, Spain*

<sup>5</sup>*Laboratoire de Chimie Théorique, UMR7616, Université P. et M. Curie-Paris 6,*

*4 Place Jussieu case 137, 75252 Paris Cedex 05, France*

(Received 2 February 2009; revised manuscript received 30 April 2009; published 4 August 2009)

We theoretically predict the occurrence of negative differential resistance (NDR) in scanning tunneling spectroscopy for a pure C<sub>60</sub> monolayer deposited on a metal surface using metal tips, namely, on a Cu(111) surface and using various W tips. It is proposed that the likely reason why NDR has not been observed under such conditions is that NDR can be reduced if an oxidized or Cu-terminated tip is used. A detailed decomposition of the total tunneling current into its contributions from individual molecular orbitals reveals that only some of the orbitals on the tip and on the C<sub>60</sub> can be “matched up” to give a contribution to the current and that the NDR is a consequence of the mismatch between these specific orbitals within particular ranges of bias voltage. Moreover, the NDR characteristics, including the peak positions and the peak-to-valley ratios, are found to depend on the tip material, tip geometry, and tip-to-molecule position.

DOI: [10.1103/PhysRevB.80.075403](https://doi.org/10.1103/PhysRevB.80.075403)

PACS number(s): 85.65.+h, 73.61.Wp, 68.37.Ef

## I. INTRODUCTION

Negative differential resistance (NDR), defined as a decrease in the electrical current with increasing voltage (within some voltage range), is a key ingredient of molecular electronic devices.<sup>1</sup> Since its realization at the molecular scale in 1999,<sup>2</sup> NDR has drawn considerable attention and has been the subject of many studies.<sup>3–7</sup> Within the context of scanning tunneling microscopy (STM) measurements, including scanning tunneling spectroscopy (STS), the origin of NDR is generally assigned to the alignment and misalignment in energy of narrow features of both the tip and the sample states as the bias is swept.<sup>8</sup>

C<sub>60</sub> molecules adsorbed on surfaces have been intensively investigated for their potential applications in molecular electronics. For these, NDR features have been observed in several STM experiments: (1) double layers or multilayers of adsorbed C<sub>60</sub> molecules;<sup>4</sup> (2) a monolayer of C<sub>60</sub> molecules on top of an insulator layer;<sup>3,9</sup> and (3) a monolayer of adsorbed C<sub>60</sub> molecules with reduced molecule-substrate coupling by codeposition of other molecules.<sup>6,7</sup> So far, no significant NDR has been reported for a pure C<sub>60</sub> monolayer on a metal surface. For the above three cases, NDR would be favored by the existence of sharp C<sub>60</sub> molecular levels due to a weak interaction between the substrate and the C<sub>60</sub>. However, this interaction is strong and broadens<sup>10,11</sup> the molecular levels, thus reducing the possibility for a negative slope in the voltage-current curve so that it is not surprising that significant NDR features are seldom observed for a pure C<sub>60</sub> monolayer on metal surfaces.

In the present study, we show that NDR features can, in fact, be obtained in a pure C<sub>60</sub> monolayer on a Cu(111) surface through the matching and mismatching between the atomic orbitals (AOs) of the tip apex atom and the molecular orbitals (MOs) of the C<sub>60</sub> molecule as the bias voltage is

changed. The NDR features revealed by theoretical STM and STS simulations is expected to lead to experimental verification. The matching and mismatching between the tip and molecular orbitals with increasing bias voltages are similar to the “local-orbital symmetry matching” proposed for the cobalt phthalocyanine (CoPc) molecule with a Ni tip.<sup>5</sup> Furthermore, our results show that the NDR characteristics, including the peak positions and the peak-to-valley ratios, are related to the tip material, tip geometry, and tip-to-molecule position.

## II. THEORETICAL MODELING AND RESULTS

Figures 1(a) and 1(b) show the atomic geometry of the C<sub>60</sub>/Cu(111) adsorption system in one (4×4) unit cell. Based on experimental observations and calculated minimum total energies,<sup>10,12,13</sup> the intact C<sub>60</sub> molecules are adsorbed on hcp hollow sites of the unreconstructed Cu(111) surface with an orientation illustrated in Fig. 1(b); these form an ordered (4×4) periodic array, as can be prepared and observed experimentally under specific conditions.<sup>12,13</sup> The structure was relaxed (in the absence of a tip) by employing the VASP (Ref. 14) code based on density-functional theory at the generalized gradient approximation level.<sup>15</sup> In addition and in order to address the role of the tip in the *I-V* characteristics, we consider different tips, varying both their chemical identity (W, Pt, or Ir) as well as their orientation—see Figs. 2 and 3 for the various tip geometries. We employ the Green’s-function-based GREEN code<sup>16,17</sup> for all STM/STS simulations assuming zero temperature. Since the code treats the sample and the tip on an equal footing, it is especially suited for explicitly addressing any tip effects.

We simulate the entire STM system at the atomic level, employing total-energy-optimized geometries for both the sample and the tips.<sup>18,19</sup> The Hamiltonian of the entire STM

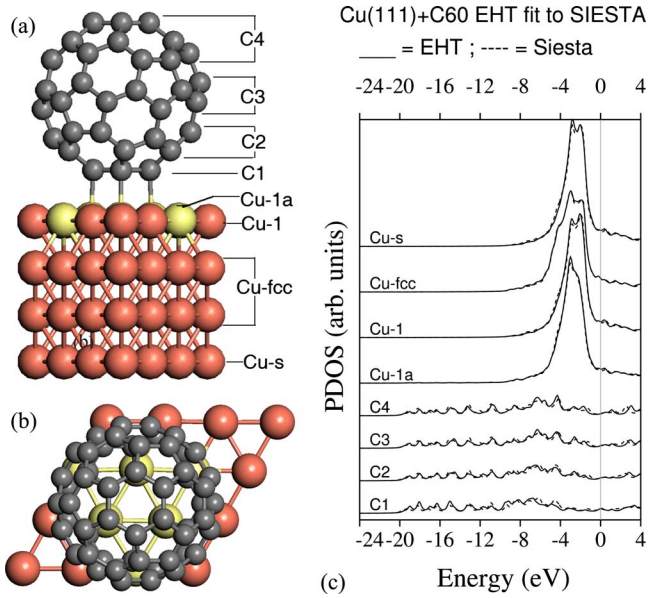


FIG. 1. (Color online) [(a) and (b)] Adsorption geometry of a  $C_{60}$  molecule on a (relaxed and unreconstructed) Cu(111) surface, in (a) side and (b) top views; only atoms in one  $(4 \times 4)$  unit cell and 4 resp. 1 layers are shown. (c) Atomic-projected DOS from SIESTA self-consistent results, compared with corresponding PDOS obtained by fitting EHT parameters to the SIESTA results. The labels refer to atomic layers and groups marked in panel (a); group Cu-1a is shown in yellow (light gray), while group Cu-1 is shown in red (dark gray).

system is described with the extended Hückel theory (EHT),<sup>20</sup> and the EHT-related parameters are obtained after fitting the EHT atom-projected density of states to the *ab initio* counterparts for both the tip and the sample.<sup>18</sup> The EHT parameterization method described in Ref. 20 has been proven to yield accurate electronic structures as we fit to the *ab initio* self-consistent results.<sup>17,21</sup> Figure 1(c) shows the result of the EHT parameterization for the  $C_{60}/\text{Cu}(111)$  combined system [fitting to the SIESTA atomic-projected density of states (DOS)]; for fitting the EHT parameters, we divide the C atoms of  $C_{60}$  into several groups as a function of their height from the surface, as denoted by C1, C2, C3, and C4 in Fig. 1(a). The Cu atoms are also divided into several groups: the top layer Cu-1, the in-between layers Cu-fcc and the bottom layer Cu-s. For the top layer Cu-1, the Cu atoms have been further divided into two groups Cu-1a (near to  $C_{60}$ ) and Cu-1 (far from  $C_{60}$ ). Figure 1(c) shows that the *ab initio* atomic-projected DOS of the  $C_{60}/\text{Cu}(111)$  combined system are well reproduced by our EHT parameterization method. The EHT parameters for the various tips are obtained in the same way as described for the sample.

Figure 2 shows simulated  $I$ - $V$  curves for  $C_{60}$  on Cu(111) with various W tips. In the simulation of the current-voltage ( $I$ - $V$ ) curves, we consider 4 lateral locations of each tip above  $C_{60}$ , as shown in Fig. 2(f). In these  $I$ - $V$  curve plots,<sup>22</sup> negative differential resistance occurs whenever such  $I$ - $V$  curves exhibit a negative slope, e.g., to the high-voltage side of peaks. We consider different tip apex geometries, ranging from a sharp (110)-oriented pyramid to a more blunt (111)-oriented pyramid, as well as a flat (110)-terminated tip ob-

tained by removing the end atom—see insets in Figs. 2(a)–2(c), respectively. Since the W tips could be oxidized or pick up a substrate atom very easily, we also simulate W(110) tips with an oxygen or a copper atom at the apex, as shown in Figs. 2(d) and 2(e). The  $I$ - $V$  curves in Figs. 2(a)–2(c) show that clear NDR features (i.e., negative slopes) are always present with these W tips and for all the tip geometries, regardless whether they are flat or sharp. The NDR peak-to-valley ratios depend on the tip geometry and the tip-to-molecule position. For the flatter W(111) tip, the shape of the  $I$ - $V$  curves is insensitive to the tip position. Interestingly, Figs. 2(d) and 2(e) show that the NDR is decreased if the oxidized or Cu-terminated W tip is used, suggesting why NDR is rarely observed experimentally despite W tips being often employed; the W tips might be oxidized or pick up substrate atoms during the measurement. Note that the absolute current value depends on the tip-to-molecule position. Generally, the largest current occurs at position 4 while the smallest current occurs at position 3.

Since Pt-Ir alloy tips are also frequently used, we also perform simulations for pure Pt(100)- and Ir(111)-oriented tips.<sup>23</sup> The simulated  $I$ - $V$  curves, shown in Fig. 3, reveal that the NDR almost disappears if the Pt(100) tip is used while it is still present in the case of a very sharp Ir(111) tip, although the occurrence is at a higher sample bias. From this and other results visible in Figs. 2 and 3 we may conclude that the NDR features—peak position and peak-to-valley ratio—depend on the tip material, tip geometry, and tip-to-molecule position.

It is known that  $C_{60}$  may reconstruct the Cu(111) surface after annealing to well above room temperature.<sup>13,24</sup> Hence we also performed simulations for  $C_{60}$  on the reconstructed Cu(111) surface with various W tips. The results (not illustrated here) indicate that, although NDR also appears, the peak-to-valley ratio is smaller than that for  $C_{60}$  on the unreconstructed surface. This is due to the fact that the  $C_{60}$ -substrate interaction is stronger for  $C_{60}$  on the reconstructed surface and hence the broadening in the  $C_{60}$  orbitals is larger than that for  $C_{60}$  on the unreconstructed surface, reducing the opportunity for negative slopes in the  $I$ - $V$  curves.

### III. MECHANISM OF NDR

To explore the origin of the predicted NDR, we decompose the total tunneling current into its contributions from individual  $C_{60}$  MOs and AOs of the last atom of the tip, in order to detect which states contribute most to the current. Since the tunneling current mainly comes from the outermost tip apex atom—for all the simulated tips, we have checked that the apex atom contributes more than 90% of the total tunneling current—we consider only the AO contributions of the tip apex atom in the analysis.

Let us first consider the W(110) tip at position 4 for Figs. 4 and 5. Figure 4 presents the decomposition into orbitals of the total tunneling current as a function of the applied bias. We include only those states that make a significant contribution. The left panel of Fig. 4 shows that the tip  $d_{z^2}$  orbital and, to a lesser extent, the  $p_z$  and  $s$  orbitals contribute sig-

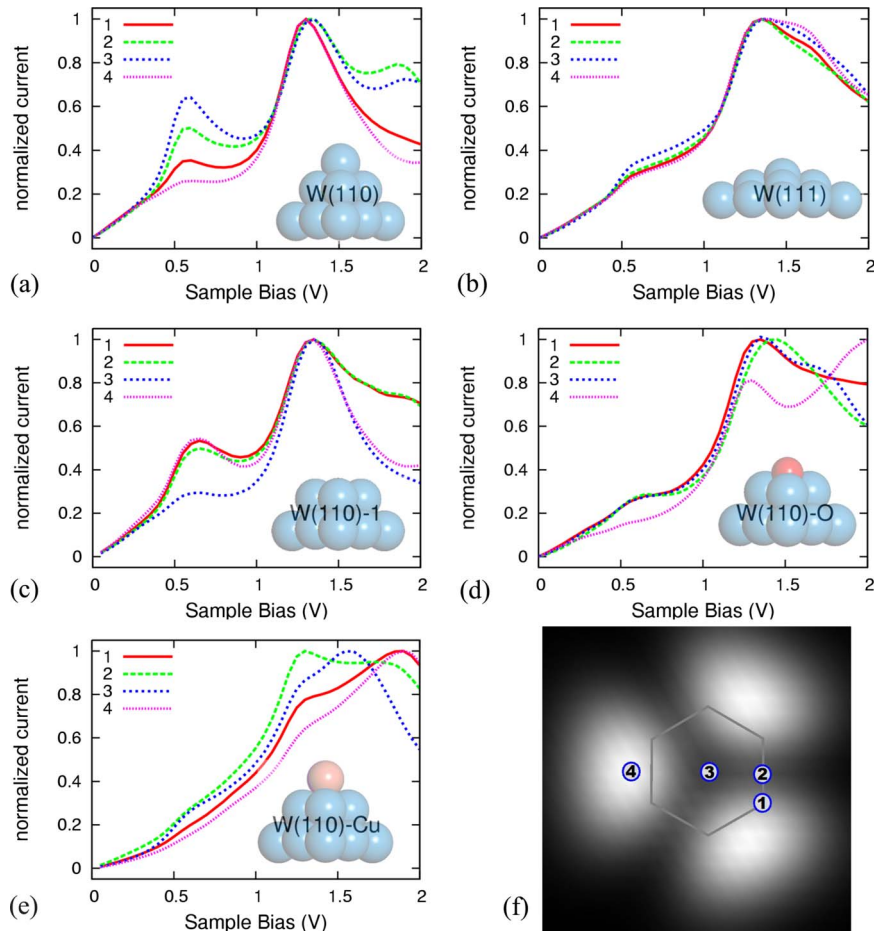


FIG. 2. (Color online) Simulated normalized  $I$ - $V$  curves of  $C_{60}$  on  $Cu(111)$  with various  $W$  tips and several tip-to- $C_{60}$  positions [positions 1, 2, 3, and 4 as shown in panel (f)]. Side views of the tip geometries are shown in each panel; in panels (a), (b), (d), and (e), the tips are pyramids, the apex atom being mostly responsible for the tunneling; in (c) the apex atom has been removed and the tunneling involves mainly four atoms; in (d) and (e) the apex atom has been replaced by an O and a Cu atom, respectively. Panels [(a)–(c)] show that NDR occurs prominently with various  $W$  tips; panels (d) and (e) show that NDR is weakened with oxidized and Cu-terminated  $W$  tips. (f) Empty local-density-of-states image for the adsorption geometry shown in Fig. 1(b). The gray hexagon indicates the top hexagonal ring of C atoms while numbers denote several lateral tip positions: position 1 places the center of the tip above one C atom, position 2 is over the center of a C-C bridge site, position 3 is over the center of the hexagonal ring, and position 4 is over the brightest point in the image (i.e., over an adjacent pentagonal ring).

nificantly to the current. On the other hand, the analysis of the  $C_{60}$  MOs reveals that only two relevant sets of orbitals are involved in the tunneling process, corresponding to the lowest virtual (i.e., unoccupied) peaks of the DOS. In the isolated  $C_{60}$  molecule, these sets correspond to unoccupied  $t_{1u}$  and  $t_{1g}$  orbitals. Upon adsorption on  $Cu(111)$ , the symme-

try is reduced to  $C_3$  and these sets split to A+E orbitals; when taking the tip into consideration, the symmetry is further reduced depending on the tip's own symmetry and position. However the splitting remains modest, especially for that arising from  $t_{1g}$ , and participates in the broadening of the DOS peaks in the adsorbed result; it is wider for the lowest

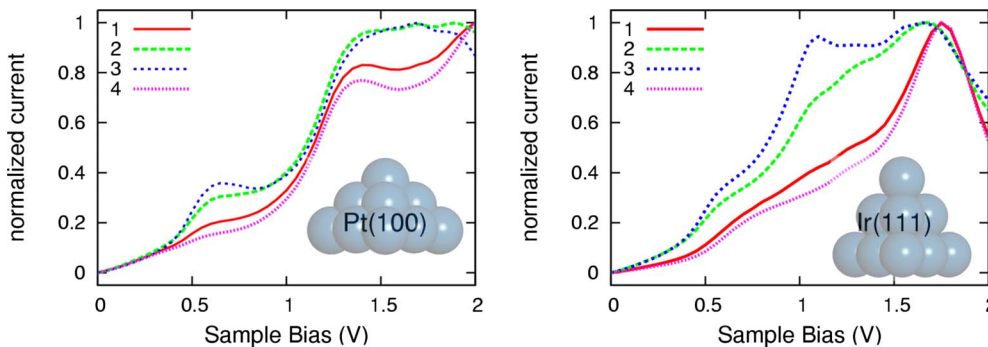


FIG. 3. (Color online) Simulated normalized  $I$ - $V$  curves of  $C_{60}$  on  $Cu(111)$  for a  $Pt(100)$  tip (left) and an  $Ir(111)$  tip (right) for various tip positions, as labeled in Fig. 2(f).



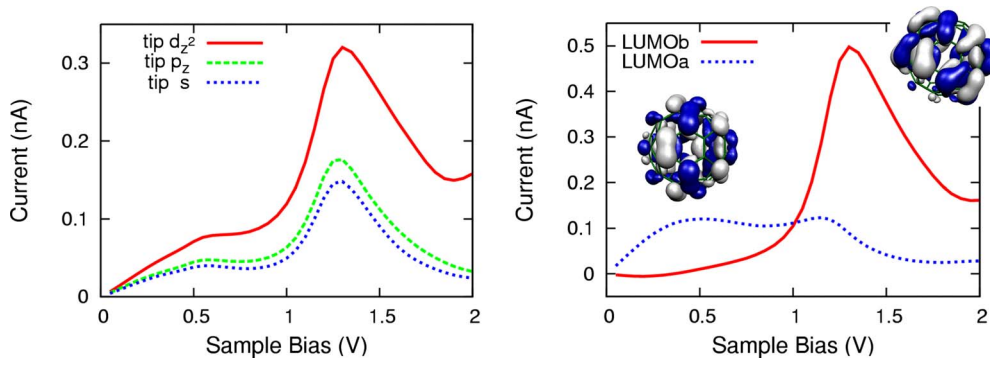


FIG. 4. (Color online) The total tunneling current decomposed according to the atomic orbitals of the tip apex atom (left) and the molecular orbitals of  $C_{60}$  (right); the corresponding molecular-orbital wave functions are also shown.

peak than for the upper peak. The tunneling involves predominantly the  $A$  orbitals, one from each set denoted hereafter lowest-unoccupied molecular orbital “a” (LUMOa) and lowest-unoccupied molecular orbital “b” LUMOb. The right panel of Fig. 4 shows the contribution of these states to the total current as well as their corresponding wave functions.

To interpret the  $I$ - $V$  characteristics, we adopt the approximation whereby the tunneling current is proportional to the energy-integrated product of the tip’s and the molecule’s projected densities of states (PDOS), after taking care of the energy shift between the two at each bias.<sup>5</sup> Accordingly, we plot in Figs. 5(a) and 5(b), respectively, the tip and molecule PDOS projected onto the states that most significantly contribute to the current. Although the PDOS for the tip  $p_z$  orbital is very small, its large spatial extension makes it more accessible to the molecule’s states and hence it makes a significant contribution to the current—see Figs. 4(a) and 5(a). For the sake of clarity, we include in Figs. 5(b)–5(d) the combined  $C_{60}$  LUMOa and LUMOb PDOS, denoted by “ $C_{60}$ -sum.”

Once the  $C_{60}$  MOs and tip AOs that contribute most to the current are identified, we can determine the origin of the NDR by examining the variation in the alignment between

these AOs and MOs at various bias voltages. The NDR appears in the positive sample bias-voltage range, for which the tip states shift up in energy relative to the adsorbed  $C_{60}$  states. To find the relative energy shift between the PDOS of the tip and of the  $C_{60}$  molecule, we fix the energy of the  $C_{60}$  LUMOs (LUMOa and LUMOb, combined and denoted by  $C_{60}$ -sum) while shifting up the energy of the tip AOs with the bias voltage. The NDR appears when the sample bias is larger than 1.3 V. At 1.3 V, the tip  $d_{z^2}$  orbital has shifted up in energy by 1.3 eV, as denoted by “1.3 V, tip  $d_{z^2}$ ” in Fig. 5(c); with even higher bias voltages, the tip  $d_{z^2}$  orbital has shifted up further. From Fig. 5(c) we can see that, at bias 1.3 V, in the energy range of 0.0–0.4 eV the broad peak of the tip  $d_{z^2}$  orbital matches the broad peak of the  $C_{60}$  LUMO. With increasing bias voltage, a mismatch between the two broad peaks appears. At 1.8 V, the broad tip peak is completely mismatched from the  $C_{60}$  LUMO. This mismatch between the broad tip peak and the  $C_{60}$  LUMO with biases higher than 1.3 V is one source of NDR. In the energy range above 1.1 eV, where the  $C_{60}$  LUMOb is located, the tip PDOS decreases with increasing bias voltage; this is another source of NDR.

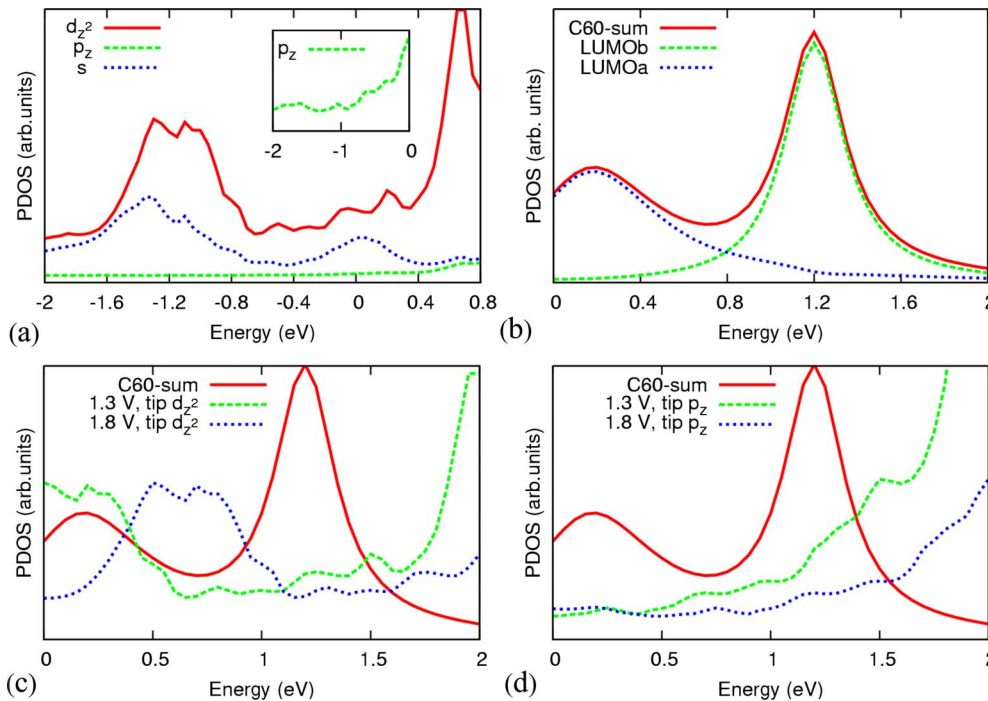


FIG. 5. (Color online) [(a) and (b)] PDOS of the tip apex AOs and the  $C_{60}$  MOs, respectively, that significantly contribute to the current (the small  $p_z$  PDOS values are magnified in the inset); the Fermi energy is set to zero; [(c) and (d)] evolution of tip  $d_{z^2}$  and  $p_z$  orbitals, respectively, relative to the  $C_{60}$  LUMOs, with increasing sample biases of 1.3 and 1.8 V.  $C_{60}$ -sum denotes LUMOa and LUMOb combined.

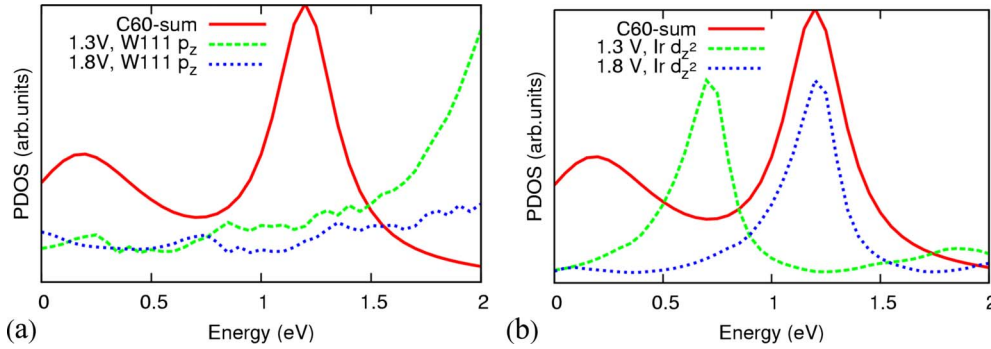


FIG. 6. (Color online) (a) The upshift of the W(111) tip  $p_z$  states and (b) the Ir tip  $d_{z^2}$  states relative to the  $C_{60}$  LUMOs with increasing bias voltages. See Fig. 5 for more details.

Thus, with a sample bias larger than 1.3 V, NDR results from the mismatch between the broad peaks of the tip  $d_{z^2}$  orbital and of the  $C_{60}$  LUMO, and from the decrease in the tip PDOS in the energy range where the  $C_{60}$  LUMO is located. Note that in Figs. 5(c) and 5(d) we scale the PDOS of the tip and the molecule differently for better visibility. The match and mismatch between the tip  $s$  orbital and the  $C_{60}$  LUMOs are similar to those of the tip  $d_{z^2}$  orbital. For the tip  $p_z$  orbital with a bias larger than 1.3 V, NDR results from the decrease in the PDOS in the energy region larger than 0.5 eV, as shown in Fig. 5(d).

The same analysis can be applied to the other tips to explain the origin of the NDR features. For the W(111) tip, the tip  $p_z$  orbital contributes most to the current while, for the Ir tip, the tip  $d_{z^2}$  orbital contributes most. Figures 6(a) and 6(b) show the evolution of the W(111) tip  $p_z$  states and Ir tip  $d_{z^2}$  states relative to the  $C_{60}$  LUMOs. For the W(111) tip with a bias larger than 1.3 V, the NDR resulting from the decrease in the PDOS occurs in the energy region above 0.7 eV. For the Ir tip, the tip  $d_{z^2}$  states match the  $C_{60}$  LUMO at 1.8 V so that the NDR appears at voltages above 1.8 V.

For the  $C_{60}$  molecule studied in this work, NDR is significant with a W tip while it almost disappears for a Pt tip; for the CoPc molecule investigated in previous work,<sup>5</sup> NDR is apparent with a Ni tip but disappears with a W tip; for the terphenylthiol molecule studied in earlier work,<sup>8</sup> NDR appears with a Pt tip. From the NDR behavior discussed in our work and in two previous publications,<sup>5,8</sup> we can draw the conclusion that the occurrence of NDR depends on the electronic structure of both the molecule and the tip. Namely, for a particular molecule, NDR tends to appear only with a suitable tip, depending on the local-DOS peak positions and local-orbital symmetries of both the tip and the molecule.

Our work indicates that the occurrence of NDR depends on two factors: (a) the relative local-DOS peak position between the tip and the sample; (b) the orbital symmetry matching between the tip and the molecule. If one only considers the local-DOS peak position, there are too many peaks in most actual systems. However, if one further considers the orbital symmetry matching between the tip and the sample, we may find that many local-DOS peaks do not contribute to the current. This is the key factor that results in NDR for adsorbed  $C_{60}$  with W tips.

#### IV. CONCLUSIONS

In summary, significant NDR features can be obtained with a pure  $C_{60}$  monolayer adsorbed on the Cu(111) surface using various W tips, owing to the match and mismatch between tip AOs and the molecule MOs with increasing biases. NDR is largely insensitive to the tip geometry, which is an important implication for its experimental realization. The easy oxidation and/or pick up of substrate atoms by the W tip, which considerably reduces NDR, would explain why significant NDR has seldom been observed experimentally with W tips, despite the frequent use of such tips. Our findings are expected to be very useful for selecting other tip materials that can present NDR.

#### ACKNOWLEDGMENTS

The work described in this paper is supported by a grant from the Research Grants Council of Hong Kong SAR (Project No. CityU 102408) and the Centre for Applied Computing and Interactive Media (ACIM). P.W.W. acknowledges support from NSC-97-2120-M-002-008, Taiwan. C.M. acknowledges the French Consulate in Hong Kong for funding through an exchange program.

<sup>1</sup>R. L. Carroll and C. B. Gorman, *Angew. Chem., Int. Ed.* **41**, 4378 (2002).

<sup>2</sup>J. Chen, M. A. Reed, A. M. Rawlett, and J. M. Tour, *Science* **286**, 1550 (1999).

<sup>3</sup>C. Zeng, H. Wang, B. Wang, J. Yang, and J. G. Hou, *Appl. Phys. Lett.* **77**, 3595 (2000).

<sup>4</sup>M. Grobis, A. Wachowiak, R. Yamachika, and M. F. Crommie, *Appl. Phys. Lett.* **86**, 204102 (2005).

<sup>5</sup>L. Chen, Z. Hu, A. Zhao, B. Wang, Y. Luo, J. Yang, and J. G.

Hou, *Phys. Rev. Lett.* **99**, 146803 (2007).

<sup>6</sup>K. J. Franke, G. Schulze, N. Henningsen, I. Fernández-Torrente, J. I. Pascual, S. Zarwell, K. Ruck-Braun, M. Cobian, and N. Lorente, *Phys. Rev. Lett.* **100**, 036807 (2008).

<sup>7</sup>I. Fernández-Torrente, K. J. Franke, and J. I. Pascual, *J. Phys.: Condens. Matter* **20**, 184001 (2008).

<sup>8</sup>Y. Xue, S. Datta, S. Hong, R. Reifenberger, J. I. Henderson, and C. P. Kubiak, *Phys. Rev. B* **59**, R7852 (1999).

<sup>9</sup>N. A. Pradhan, N. Liu, and W. Ho, *J. Phys. Chem. B* **109**, 8513

- (2005).
- <sup>10</sup>L.-L. Wang and H.-P. Cheng, *Phys. Rev. B* **69**, 045404 (2004).
- <sup>11</sup>F. Schiller, M. Ruiz-Osés, J. E. Ortega, P. Segovia, J. Martínez-Blanco, B. P. Doyle, V. Pérez-Dieste, J. Lobo, N. Néel, R. Berndt, and J. Kröger, *J. Chem. Phys.* **125**, 144719 (2006).
- <sup>12</sup>Tomihiko Hashizume, K. Motai, X. D. Wang, H. Shinohara, Y. Saito, Y. Maruyama, K. Ohno, Y. Kawazoe, Y. Nishina, H. W. Pickering, Y. Kuk, and T. Sakurai, *Phys. Rev. Lett.* **71**, 2959 (1993).
- <sup>13</sup>W. W. Pai, C.-L. Hsu, M. C. Lin, K. C. Lin, and T. B. Tang, *Phys. Rev. B* **69**, 125405 (2004); W. W. Pai, C. L. Hsu, K. C. Lin, and T. B. Tang, *Appl. Surf. Sci.* **241**, 194 (2005).
- <sup>14</sup>G. Kresse and J. Furthmüller, *Comput. Mater. Sci.* **6**, 15 (1996).
- <sup>15</sup>J. P. Perdew and Y. Wang, *Phys. Rev. B* **45**, 13244 (1992).
- <sup>16</sup>J. Cerdá, M. A. Van Hove, P. Sautet, and M. Salmeron, *Phys. Rev. B* **56**, 15885 (1997); J. Cerdá, A. Yoon, M. A. Van Hove, P. Sautet, M. Salmeron, and G. A. Somorjai, *ibid.* **56**, 15900 (1997).
- <sup>17</sup><http://www.icmm.csic.es/jcerda/>
- <sup>18</sup>We used the SIESTA code (Ref. 19) to relax the various tip structures; the EHT parameters are then fitted to the SIESTA atom-projected density of states.
- <sup>19</sup>J. M. Soler, E. Artacho, J. D. Gale, A. García, J. Junquera, P. Ordejón, and D. Sánchez-Portal, *J. Phys.: Condens. Matter* **14**, 2745 (2002).
- <sup>20</sup>J. Cerdá and F. Soria, *Phys. Rev. B* **61**, 7965 (2000), and references therein.
- <sup>21</sup>D. Kienle, J. I. Cerdá, and A. W. Ghosh, *J. Appl. Phys.* **100**, 043714 (2006); D. Kienle, K. H. Bevan, G. C. Liang, L. Siddiqui, J. I. Cerdá, and A. W. Ghosh, *ibid.* **100**, 043715 (2006).
- <sup>22</sup>In the calculation of the current, the tip-sample vertical distance (perpendicular to the surface) is about 5.2 Å and the maximum absolute current value changes from several tenths of nano-Amperes for the W tips to several nano-Amperes for the Pt tip. Also, the absolute current value depends on the tip-to-molecule position. Generally, the largest current occurs at position 4 while the smallest current occurs at position 3. We have checked that the influence of the distance (from 5.2 Å to 6.2 Å) on the shape of the *I-V* curve is not significant.
- <sup>23</sup>Since the atomic structure is unknown for Pt-Ir alloy tips, we only simulated pure Pt and pure Ir tips.
- <sup>24</sup>Woei Wu Pai *et al.* (unpublished).